

# Polymorphism of crystalline phases of calcium stearate

P. GARNIER, P. GREGOIRE

*Ecole Centrale de Paris, Laboratoire de Chimie-Physique du Solide, UA CNRS 453, Grande Voie des Vignes, 92295 Chatenay-Malabry Cédex, France*

P. MONTMITONNET, F. DELAMARE

*Ecole des Mines de Paris, Centre de Mise en Forme des Matériaux, UA CNRS 852, Sophia-Antipolis, 06565 Valbonne Cédex, France*

The structures of the low temperature ( $T \leq 400$  K) phases of calcium stearate have been investigated by X-ray diffraction. Several forms are shown to exist at room temperature, depending on hydration and thermal treatment. New transitions at cryogenic temperatures are discussed. Transitions at higher temperatures have been investigated together with their reversibility. Thermogravimetry and two calorimetric techniques have been used as a complement. This data completes the already somewhat complex picture of the phase transitions of calcium stearate.

## 1. Introduction

Calcium stearate  $(\text{CH}_3-(\text{CH}_2)_{16}-\text{COO})_2\text{Ca}$  is a metal soap commonly used as a lubricant for diverse processes. Its most important uses are in polymer extrusion (PVC or propergols) and metal forming (wire drawing). Moreover, calcium stearate is one of the major bases for greases.

Its lubricating action is intimately related to its rheology which in turn depends on its structure. As most soaps, calcium stearate exhibits several thermotropic crystalline, then mesomorphic phase transitions [1]. The structures of these phases have been studied [2-4] by X-ray diffraction. However, it has been shown that the room temperature structure is extremely sensitive to both purity and thermal treatments [5], such as those accompanying soapmaking.

More precisely, two crystalline phases are encountered up to 373 K, then between 373 and 396 K, respectively termed C1 and C2 [3]. In the present paper, only this temperature range will be investigated. The structures are sketched in Fig. 1: the polar parts  $(\text{COO})_2\text{Ca}$  are gathered in planes between which the fatty chains are extended. Hence, the interlayer spacing  $d$  is approximately twice the length of a molecule. A wide range of values are given in the literature for  $d$  (Table I) at room temperature. Vold *et al.* [5] have shown that these discrepancies in part result from different degrees of hydration: 5.04 nm corresponds to anhydrous calcium stearate, whereas 4.95 nm is a monohydrate [6]. The difference between [3] and [7] is probably due to experimental uncertainties and/or sample purity (the product of [3] is much purer). Moreover, it can be found [5] that calcium stearate heated up to 500 K or more, then rapidly cooled to room temperature, has a  $d$  value of 4.85 nm. Fig. 2 [5] shows that several room temperature phases (or crystalline states) may be found depending on the

maximum temperature of prior heating. However, 4.73 nm (Table I) is never found in this study, and must correspond to an impure soap. As for in-plane order, little is known. The C2 X-ray diagram is said to be consistent with hexagonal packing [3].

In the present paper, we propose a more detailed structural investigation of the phases encountered below 396 K. The influence of thermal treatments below 396 K will be described. Contrary to previous works, this study has been extended to low temperatures (down to 100 K).

## 2. Experimental techniques

### 2.1. Preparation of soaps

Two soaps (A and B) from different stearic acids have been prepared using different techniques. Soap A was derived from a solution containing 95.1% stearic acid (C18), 3.1% palmitic acid (C16), 0.6% arachidic acid (C20) and 1.2% oleic acid (unsaturated C18). The corresponding soap impurities are miscible with calcium stearate, hence the structures are not greatly modified [8]. The acid was saponified by  $\text{Ca}(\text{OH})_2$  in a reactor. The exothermic character of this reaction causes the soap to be prepared at about 480 K hence, soap A not only contains impurities, but it has also undergone a thermal treatment.

Soap B is from an ultra-pure (> 99.5%) FLUKA stearic acid, saponified by a stoichiometric quantity of  $\text{Ca}(\text{OH})_2$  in alcohol (double precipitation technique),

TABLE I Interlayer spacing of calcium stearate at 293 K

Reference	$d$ (nm)
[2]	4.73
[3]	5.06
[6]	4.95
[7]	5.04

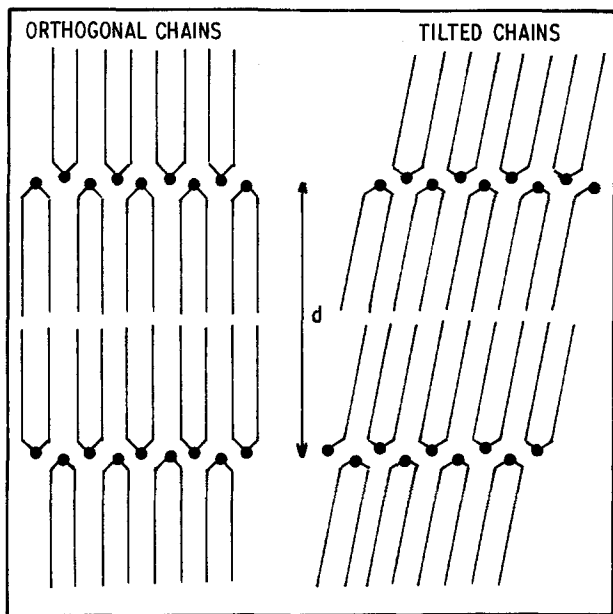


Figure 1 Schematic picture of crystalline phases of calcium stearate. Black circles represent the Ca cations.

and has hence never undergone heat changes before the study. Thermogravimetry has shown that these soaps are monohydrates. Whenever desired, dehydration is done slightly below 373 K to avoid any phase transition, under vacuum ( $\approx 10^{-2}$  atm.).

## 2.2. X-ray diffraction apparatus

X-ray diffraction diagrams on polycrystalline samples have been obtained using a prototype two-axis goniometer [9] and a rotating anode generator of 12 kW. The angular precision is  $10^{-3} \theta$ . For the low temperature study, the samples are placed in a He-cryostat cooled by gaseous conduction. The thermal stability is 0.03 K, the precision of the measurement is 0.1 K. High temperature studies have been performed in a RIGAKU furnace with a stability of 1 K and a precision of 2 K. Throughout the present study, the wavelength  $\lambda = 0.154178$  nm was utilized.

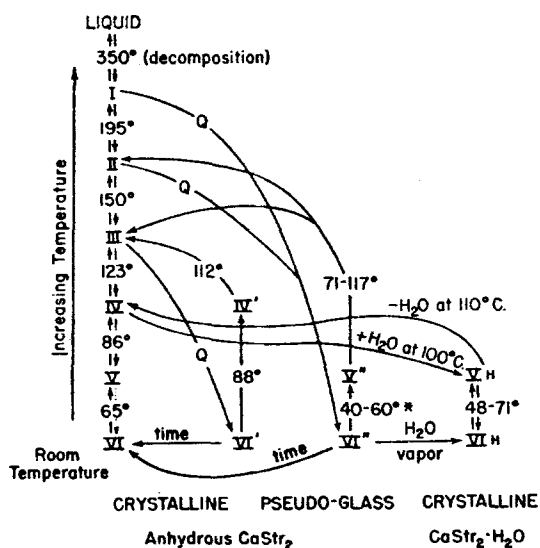


Figure 2 Irreversibility of thermotropic phase transitions of calcium stearate and calcium stearate monohydrate [5]. (Q) quenching, (\*) heat evolved.

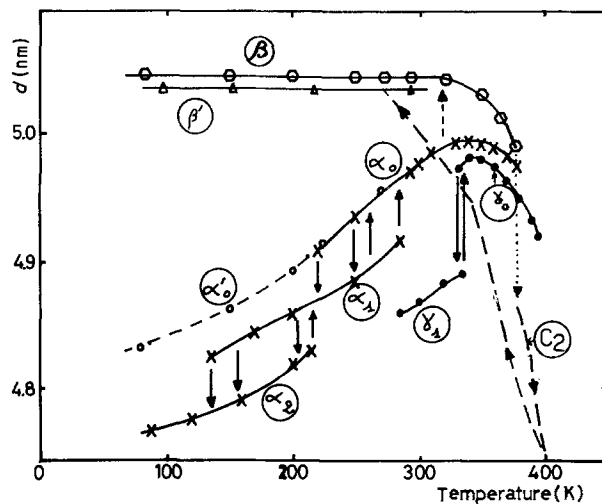


Figure 3 Synoptic diagram of low temperature transitions of calcium stearate determined by X-ray measurement of interlayer spacing  $d$ : ( $\uparrow$ ) ( $\downarrow$ ) arrows indicate heating or cooling, ( $- \rightarrow$ ) effect of thermal treatment.

## 2.3. Calorimetric experiments

Two types of apparatus were used. First one is a PERKIN-ELMER DSC IIB differential scanning calorimeter. Temperature and enthalpy calibrations were made using the melting peak of indium samples ( $T_m = 429.7$  K,  $\Delta H = 28.4$  J g $^{-1}$ ). Samples (5–10 mg) were placed in open pans to allow for any possible water loss.

The second apparatus is a SETARAM DSC 111 differential scanning calorimeter in which the sample and reference are entirely surrounded by the heat flux transducers. Calibration is achieved during manufacturing of the apparatus by Joule heating of a special specimen. The minimum temperature is 150 K.

## 3. The different types of structures

All crystalline phases are characterized by a well defined interlayer distance  $d$ . The different phases and phase transitions have been evidenced by measuring  $d$  by X-ray diffraction. Eleven harmonics are easily seen with sharp peaks (full width at half maximum  $\Delta\theta \approx 0.05^\circ \theta$  for  $\theta \approx 5^\circ$ ), which indicates a good crystalline order along this direction.

Fig. 3 is a summary of the phases and transitions encountered during this study, which are described hereafter. Four families of phases may be distinguished. One at high temperature ( $377$  K  $< T < 395$  K) obviously corresponds to the C2 phase of

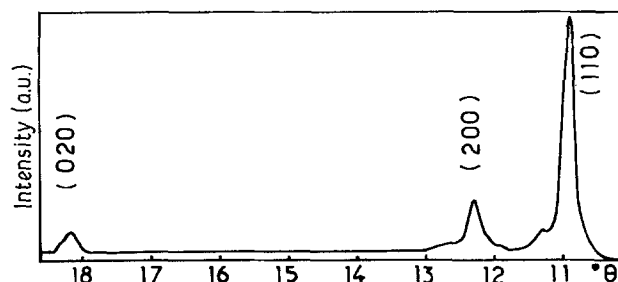


Figure 4 Powder diffraction diagram of phase  $\beta$  at 293 K. Miller's indices correspond to the supposed orthorhombic cell.

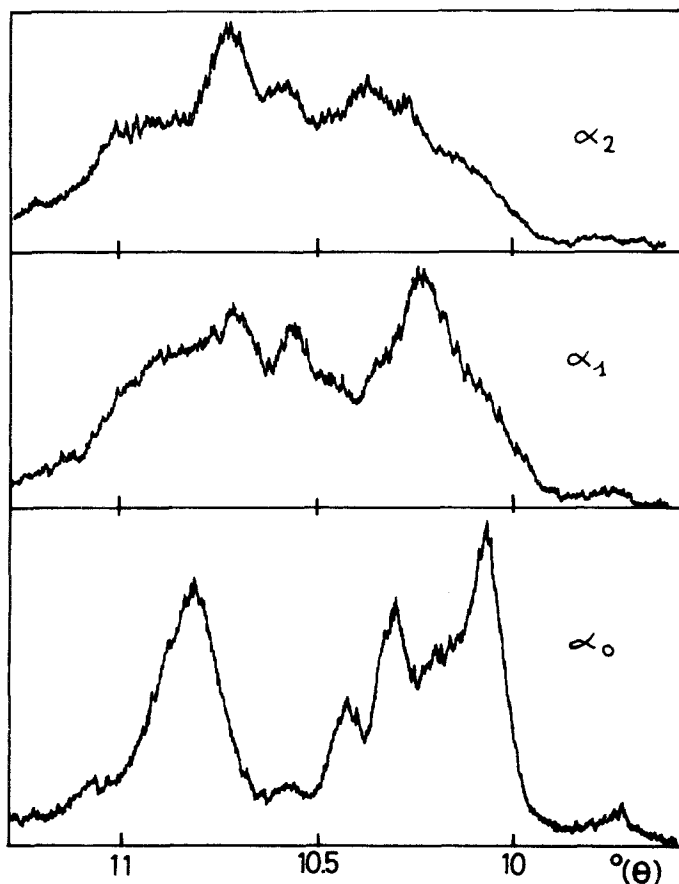


Figure 5 Comparison of the powder diffraction diagram of  $\alpha$  phases.

Spagt [3]. The other 3 families (termed here  $\alpha$ ,  $\beta$ ,  $\gamma$ ) are several forms existing at low temperature, their occurrence depending on thermal treatments.

### 3.1. The $\beta$ phases

The  $\beta$  phase is the normal state of ultra-pure soap B. Interlayer distance  $d$  is 5.048 nm, which corresponds to extended chains normal to the polar planes [3]. This distance is practically independent of temperature between 100 K and 330 K. Hence, thermal expansion is limited to in-plane distances. Above 330 K, although no global structural changes are observed,  $d$  begins to decrease slowly.

In-plane order is illustrated in Fig. 4. Sharp peaks reveal a well established in-plane order. It has been possible to index this diagram with the orthorhombic cell previously observed for lead stearate [10, 11]. Only the first (1 1 0), (2 0 0) and (0 2 0) peaks are observed. Some undulations and a small peak ( $\theta \approx 11.3^\circ$ ) are sometimes observed; they are probably due to diffuse scattering characterizing distortion and impurities. The proposed indexation is however confirmed by its consistence with thermal expansion, i.e. the indexation is correct at all temperatures. The experimental thermal expansion coefficients are:  $\alpha_{200} = 58.5 \cdot 10^{-6} \text{ K}^{-1}$  and  $\alpha_{020} = 111.0 \cdot 10^{-6} \text{ K}^{-1}$ ; the deduced  $\alpha_{110}$  is  $79 \cdot 10^{-6} \text{ K}^{-1}$ , whereas the observed value is  $75 \cdot 10^{-6} \text{ K}^{-1}$ . The cell parameters at 294 K are  $a = 0.498 \text{ nm}$ ,  $b = 0.728 \text{ nm}$  and  $c = d = 5.048 \text{ nm}$ .

Under certain circumstances (thermal treatments) a slightly different form  $\beta'$  ( $d = 5.037 \text{ nm}$ ) can be observed. It has obviously a poorer in-plane order, but still corresponds to the same type of structure.

### 3.2. The $\alpha$ phases

This is the usual state of our less pure, monohydrate soap A. Three  $\alpha$  phases are successively encountered when temperature decreases:  $\alpha_0$ ,  $\alpha_1$ ,  $\alpha_2$ . Phases  $\alpha_2$  and  $\alpha_1$  coexist on a large temperature range (208 to 218 K on heating). The same is true for  $\alpha_1$  and  $\alpha_0$  between 263 and 293 K, which proves that these are first order transitions. Moreover, they exhibit a high hysteresis

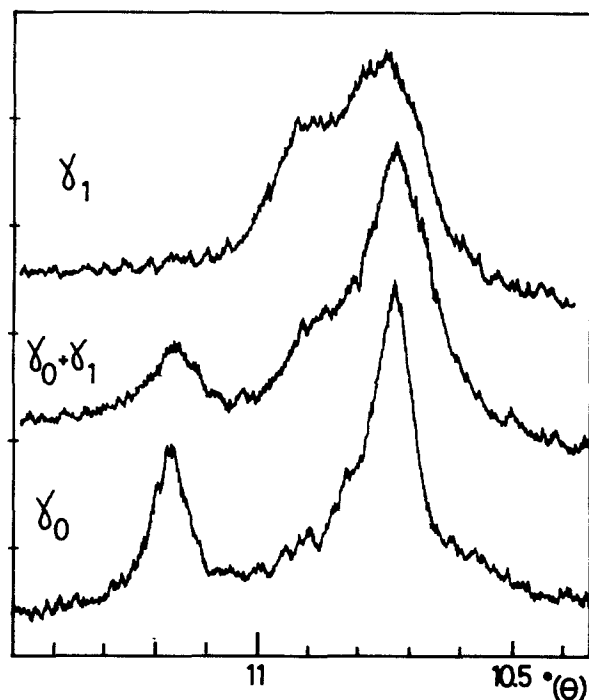


Figure 6 Powder diffraction diagram of  $\gamma$  phases, showing the  $\gamma_1$ - $\gamma_0$  transition.

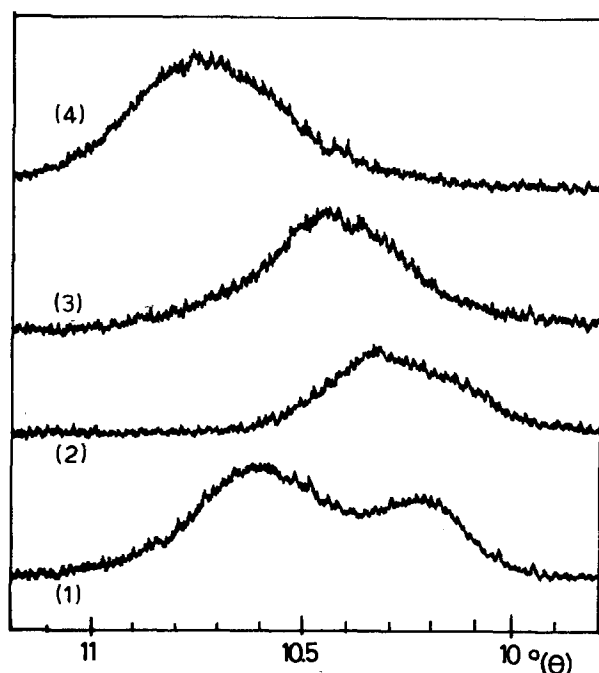


Figure 7 Powder diffraction diagrams of phases C2 and undercooled C2 (1) C2 just at the transition: 376 K on heating (2) C2 after further heating to 394 K (3) Undercooled C2 after cooling down to 376 K (note the single peak) (4) phase  $\beta'$  resulting from cooling C2 under 338 K.

( $\Delta T = 60$  K for  $\alpha_2 \rightarrow \alpha_1$ ,  $\Delta T = 30$  K for  $\alpha_1 \rightarrow \alpha_0$ ). These transitions had never been reported previously. Phase  $\alpha_0$  is the stable form at room temperature.  $d$  is lower (4.975 nm) than in the  $\beta$  phase, which indicates that the chains are tilted with respect to the planes. When temperature increases,  $d$  goes through a maximum at 343 K ( $d_{\max} = 4.997$  nm). The in-plane diagrams are shown in Fig. 5. Phase  $\alpha_0$  has a lower symmetry than the  $\beta$  phase, monoclinic or triclinic cell. This is consistent with tilted molecules. Up to now, indexing of this diagram could not be performed, by lack of data from a single crystal. Phases  $\alpha_1$  and  $\alpha_2$  are probably poorly crystallized, as shown by the unresolved peaks between 10 and  $11^\circ \theta$ .

Note that a cooling run after thermal treatment (313 K during 1 h) has given a phase  $\alpha'_0$ , similar to  $\alpha_0$  at room temperature, but which does not undergo the  $\alpha_1$  and  $\alpha_2$  transitions. It is probably a partially dehydrated form. It is very difficult to obtain this pure phase, but it is frequently observed at low temperature (77 K) as small quantities mixed with  $\alpha_2$  or  $\beta$  phases. The  $\alpha'_0$  in-plane diagram is similar to  $\alpha_2$ , and the two phases differ only by the value of  $d$  (Fig. 3).

### 3.3. The $\gamma$ phases

These are encountered for soap A only after thermal treatment, probably because of dehydration. The  $\gamma$  phases are characterized by the lowest interlayer spacing ( $d = 4.866$  nm at 294 K).  $\gamma_1$  is the stable form at room temperature, and undergoes a reversible transition at  $\approx 338$  K toward a  $\gamma_0$  phase; again, this transition had not been reported before.  $\gamma_0$  has a maximum  $d$  value at 343 K (4.985 nm). It persists until 396 K, without transition towards C2.

As for in-plane order,  $\gamma_0$  is characterized by two peaks at  $10.75^\circ \theta$  and  $11.2^\circ \theta$ . During the transition towards  $\gamma_1$ , these peaks tend to overlap (Fig. 6). Interpretation of this diagram has not been possible up to now.

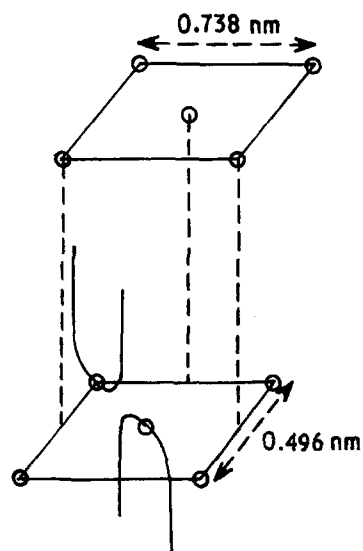


Figure 8 Position of the stearate chains within unit cell as proposed by [10] for lead stearate.

### 3.4. The 377–396 K range: C2 phase

At 377 K, phases  $\beta$  and  $\alpha$  undergo a transition towards what is obviously a C2 phase [3]. In this phase,  $d$  varies rapidly, contrary to the results of Spect [3]. Fig. 7 gives the in-plane diagram, with a single, broad peak at  $\approx 10.6^\circ \theta$ , with a shoulder at low angles (curve 1). This peak has been interpreted as indicating hexagonal packing [3], but the existence of the shoulder proves that reality is probably more complex.

On cooling a sample from this phase, C2 is still found at temperatures much below 377 K, down to 338 K. Line 3 of Fig. 7 shows that the peak is then sharper and does not display any shoulder. On further cooling, the  $\beta'$  phase appears (curve 4).

## 4. Discussion of the transitions

### 4.1. The $\beta \rightarrow$ C2 transition

The  $\beta$  phase must be regarded as the standard state of pure, anhydrous calcium stearate. It corresponds to the C1 phase [3]. The interlayer distance is 5.048 nm instead of 5.06 nm, which may be attributed to experimental uncertainties. As discussed previously, the unit cell is orthorhombic with parameters  $0.494 \times 0.728 \times 5.048$  nm at 293 K, which is common for substances with long  $\text{CH}_2$  chains: the same type of structure has been found for lead stearate. However, the precise position of the chains within the unit cell is still controversial [10, 11]; Fig. 8 shows a possible configuration.

At 377 K, transition of  $\alpha$  and  $\beta$  (not  $\gamma$ ) towards the C2 phase is found. Here, we accept at the moment the hexagonal packing with interchain distance of 0.425 nm and interlayer spacing of 4.875 nm at 377 K. The shortening of  $d$  is probably not due to tilting, but rather to high conformational disorder within each chain. In [3],  $d$  was found to be constant in C1 then in C2. We have found that  $d$  is almost constant in C1 up to 343 K, then decreases (pretransitional phenomenon) from 5.048 nm at 343 K to 5.00 nm just before the transition. In the C2 phase,  $d$  decreases very rapidly: in the range 377 to 396 K,  $\alpha = 1180 \text{ } 10^{-6} \text{ K}^{-1}$ . This is at variance with [3], but is in

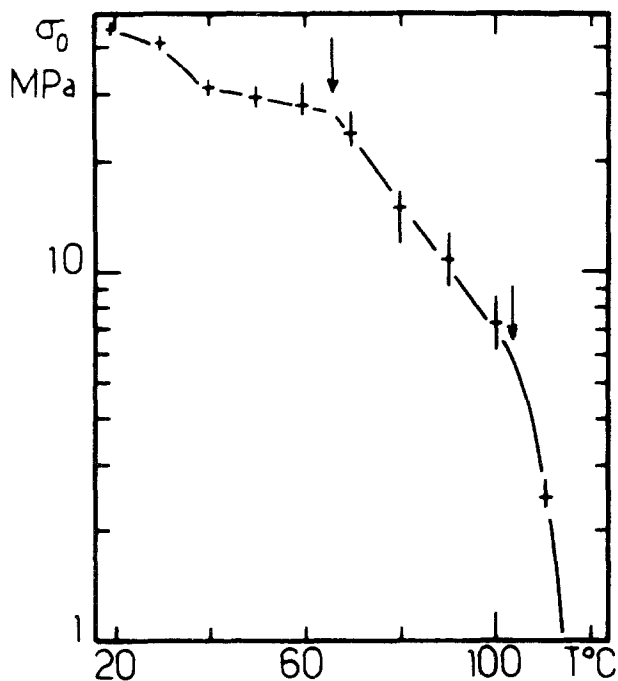
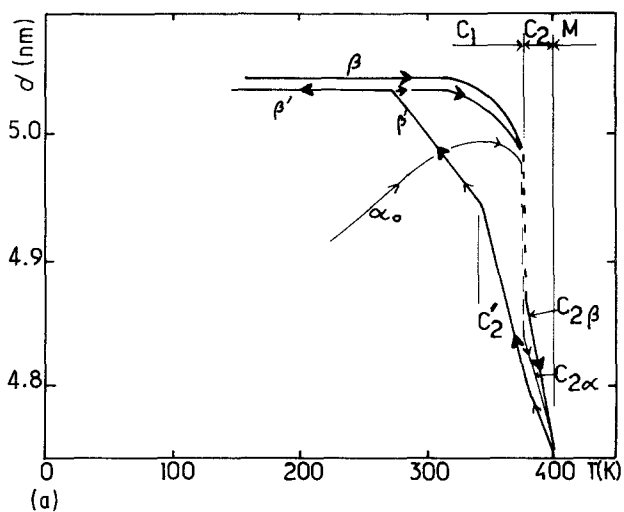


Figure 9 Variation of yield stress with temperature measured by an indentation test [14]; the initial state of the soap (A) is  $\beta'$  (dehydrated). Note the slope changes at  $\approx 335$  K (= pretransitional effect) and the fall after 377 K (transition to C2).

accordance with our own rheological study of calcium stearate [12, 13] which shows a rapid evolution of the yield stress and elastic modulus with temperature in the C2 range (Fig. 9, [14]).

On cooling from C2 (even slowly), the  $\beta'$  phase is found after a long interval (377 to 338 K) where an undercooled C2 phase exists (Fig. 10a). This irreversibility is confirmed by our DSC experiments (Fig. 10b): on a 293  $\rightarrow$  386  $\rightarrow$  293 K thermal cycle, a sharp transition is found on heating, whereas a broad peak exists on cooling between 383 and 338 K.

$\beta'$  is a modified form of  $\beta$ . The X-ray diagram shows that the difference probably does not lie in tilting with respect to the planes, but in poor crystallization resulting from a small conformational disorder.



#### 4.2. The $\alpha_2 \rightarrow \alpha_1 \rightarrow \alpha_0 \rightarrow$ C2 transitions

Hence in  $\beta$  phases chains are orthogonal to the planes, whilst chains are tilted in  $\alpha$  phases. Thermogravimetry (Fig. 11) confirms that these phases are in fact monohydrate, as was suggested by  $d = 4.975$  nm at 294 K for  $\alpha_0$ , analogous to Vold *et al.* [5] for the monohydrate. In this group, two new phases  $\alpha_1$  and  $\alpha_2$  have been discovered: chains are tilted more as temperature decreases. Note that the in-plane order is significantly improved when going from  $\alpha_2$  to  $\alpha_0$ . Then at about 340 K, conformational disorder suddenly increases, as for  $\beta$ , which results in a maximum in the  $d(T)$  curve. This is close to 343 K, the melting temperature of stearic acid ("genotypic point").

The low temperature  $\alpha_2 \rightarrow \alpha_1$  and  $\alpha_1 \rightarrow \alpha_0$  transitions must involve thermodynamic changes. This has been evidenced for the latter by DSC. Fig. 12 shows that a small peak appears on a sample cooled down to  $T_c = 151$  K, when slowly reheated. The temperature of this peak (292 K) is consistent with  $\alpha_1 \rightarrow \alpha_0$  given by X-ray diffraction. Its enthalpy is  $2.45 \pm 0.2$  J g $^{-1}$ . This transition is very sensitive to  $T_c$  and the time the soap is maintained at  $T_c$ , which confirms the broad temperature range of this transition and its slow kinetics.

$\alpha_0$  has a transition toward a C2 phase which is slightly different from that coming from  $\beta$  (Fig. 10a). However, on subsequent cooling, the same undercooled C2 phase and the same transition towards  $\beta'$  is found. This shows that such a heating run has dehydrated the sample, which will then display a stable  $\beta' \rightarrow$  C2  $\rightarrow$  undercooled C2  $\rightarrow$   $\beta'$  reversible phase sequence. The enthalpy of the  $\beta \rightarrow$  C2 transition is 13 J g $^{-1}$ .

#### 4.3. The $\gamma_0 \rightarrow \gamma_1$ transition

As for the  $\gamma$  phases, they are observed only as a result of thermal treatment of  $\alpha$ . They also exhibit a maximum interlayer distance  $d$  at 345 K. The main feature of these phases is the absence of the transition to C2 at 377 K. Fig. 13 shows the calorimetric evidence for the  $\gamma_0 \rightarrow \gamma_1$  transition, the enthalpy of which is  $6.5 \pm 1.5$  J g $^{-1}$ .

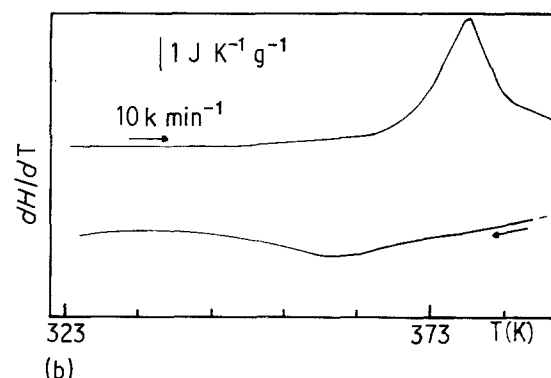


Figure 10 Irreversibility of the C1  $\rightarrow$  C2 transition (a) transformation of  $\beta$  and  $\alpha$  into C2 followed by X-ray diffraction; note the difference between C2 $\alpha$  and C2 $\beta$ . (b) Calorimetric evidence of the irreversibility (scanning rate: 10 K min $^{-1}$ )

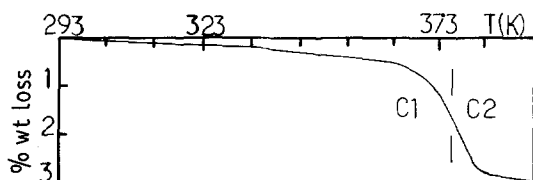


Figure 11 Thermogravimetric evidence of the monohydrate character of  $\alpha$  phases (monohydrate =  $18/624 = 2.9\%$   $\text{H}_2\text{O}$  by weight).

#### 4.4. Transformation between $\alpha$ , $\beta$ , $\gamma$ : thermal treatments

Hydrated form  $\alpha_0$  can be transformed into a mixture of  $\beta$  and  $\gamma$  by thermal treatment below 377 K. However, the proportion of  $\gamma$  and  $\beta$  varies (Table II). By heating below 343 K, a mixture about 60%  $\beta$ –40%  $\gamma$  appears; otherwise, transformation into  $\beta$  is almost complete. A pure  $\gamma$  phase is very rarely obtained. However, precise correlation with dehydration temperature or time of treatment is not possible; only tendencies can be described, as heterogeneities and impurities in the  $\alpha$  phase probably play an important part.

With the help of [5], the influence of thermal history can be extended to higher temperatures. Transitions to mesomorphic phases exist at 396, 423 and 468 K. When quenching samples from high temperatures, one obtains several different phases:

1. The phase obtained by quenching from 396 K <  $T_q$  < 423 K looks much like the  $\beta$  phase (Fig. 14); hence, contrary to Vold [5], quenching does not retain the high temperature structure.

2. If  $T_q > 423$  K, the in-plane diagram is quite similar to that of  $\gamma_1$  or  $\beta'$  (a broad peak at about 0.415–0.420 nm). For  $T_q$  between 423 and 500 K, the interlayer spacing ( $d \approx 5$  nm) is consistent with a  $\beta'$  phase; above 500 K,  $d \approx 4.85$  nm is reminiscent of  $\gamma_1$ . The critical temperature of 500 K is not consistent with any known phase transition (the last one appears at 470 K).

#### 5. Conclusion

Calcium stearate below 377 K, in the C1 phase range, exhibits one monohydrate  $\alpha$  phase, and two anhydrous forms: orthorhombic  $\beta$  phase and  $\gamma$  (undetermined structure). Within these groups, thermotropic phase transitions have been discovered: two in the  $\alpha$  group at about 210 K and 270 K, one in the  $\gamma$  group at 338 K. Moreover, dehydration of  $\alpha$  leads to a mixture of  $\beta$  and  $\gamma$ , the proportion of which depends on the dehydration temperature and probably on sample

TABLE II Transformation of  $\alpha$  into  $\beta$  and  $\gamma$  after thermal treatments

Furnace temperature (K)	Length of treatment (h)	Proportion	
		$\beta$	$\gamma$
314	70	60%	40%
325	85	55%	45%
336	80	55%	45%
343	500	100%	0%
357	90	100%	0%
363	150	90%	10%

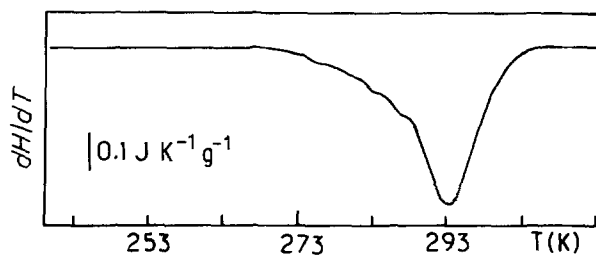


Figure 12 Calorimetry of  $\alpha_1 \rightarrow \alpha_0$  phase transition; scanning rate:  $5 \text{ K min}^{-1}$ .

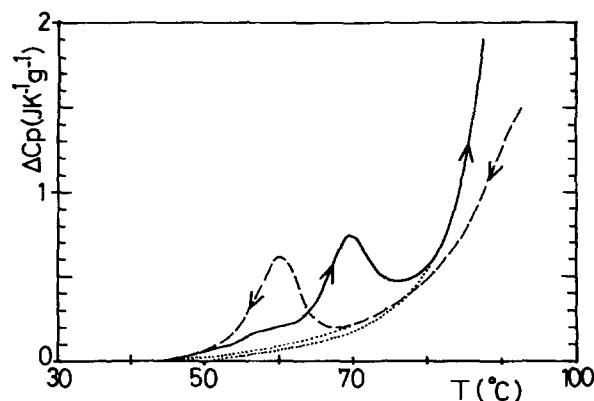


Figure 13 Calorimetry of  $\gamma_1 \rightarrow \gamma_0$  phase transition; (sample maintained 85 h at 325 K). (—) heating, (---) cooling, (····) base line.

heterogeneities.  $\gamma$  also seems to be obtained by quenching from between 396 and 423 K.

For all these phases, 343 K is an important temperature. This “genotypic point” corresponds to the melting of stearic acid. At 343 K, the conformational disorder of the chains suddenly increases, leading to poorer in-plane order (cf. our rheological results, Fig. 9) much before the C1  $\rightarrow$  C2 transition.

This last transition has been found to be only partly reversible, since an undercooled C2 phase exists down to 338 K; then in all cases,  $\beta'$  (poorly crystallized  $\beta$ ) is found, whatever the initial state  $\alpha$  or  $\beta$ . Such undercooling is quite common for mesomorphic phases of soaps [15, 16], but had never been noticed for transitions between crystalline phases of soaps.

Finally, the polymorphism demonstrated in this

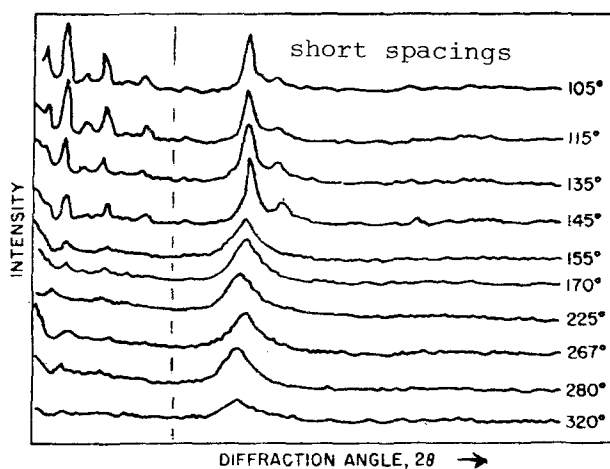


Figure 14 X-ray diffraction diagrams of calcium stearate samples quenched at various temperatures ( $^{\circ}\text{C}$ ) [5].

paper explains the various results found in the literature for the room temperature interlayer spacing of calcium stearate.

### Acknowledgements

The authors wish to thank Condat S.A. for supplying the soaps.

### References

1. G. S. HATTIANGDI, M. J. VOLD and R. D. VOLD, *Ind. Eng. Chem.* **41** (1948) 2320.
2. R. D. VOLD and G. S. HATTIANGDI, *ibid.* **41** (1949) 2311.
3. P. SPEGT, PhD thesis, Université de Strasbourg, France (1964).
4. V. LUZZATI, A. TARDIEU, T. GULYK-KRZYWICKI, *Nature* **21** (1970) 1028.
5. R. D. VOLD, J. D. GRANDINE and M. J. VOLD, *J. Colloid Sci.* **3** (1948) 339.
6. G. H. SMITH and S. ROSS, *Oil and Soap* **23** (1946) 1977.
7. M. J. VOLD and R. D. VOLD, *J. Am. Oil Chemist's Soc.* **26** (1949) 520.
8. D. DERVICHIAN and F. LACHAMPT, *Bull. Soc. Chim. Fr.* **12** (1946) 189.
9. J. F. BERAR, G. CALVARIN and D. WEIGEL, *J. Appl. Crystallogr.* **13** (1980) 201.
10. M. PRAKASH, J. B. DENG, J. B. KETTERSON and P. DUTTA, *Chem. Phys. Letters* **128** (1986) 354.
11. J. F. STEPHENS and C. TUCK-LEE, *J. Appl. Cryst.* **2** (1969) 1.
12. P. MONTMITONNET and F. DELAMARE, *J. Mat. Sci.* **17** (1982) 121.
13. *Idem.*, in Proceedings of the Conference EUROTRIB 85, T.I (Elsevier 1985).
14. P. MONTMITONNET, PhD thesis, Université de Besancon, France (1985).
15. P. MONTMITONNET, B. MONASSE, J. M. HAUDIN and F. DELAMARE, *J. Thermal Anal.* **26** (1983) 117.
16. *Idem.*, *Mat. Letters* **3** (1985) 98.

*Received 10 September  
and accepted 10 December 1987*